Cyclotron Resonance in Bismuth with a Slightly Anomalous Skin Effect

L. C. HEBEL
Bell Telephone Laboratories, Murray Hill, New Jersey
(Received 27 January 1965)

The power absorption coefficient is calculated for microwave radiation propagating normal to the surface of a slab of bismuth with a static magnetic field parallel to the sample surface where a slightly anomalous skin-effect condition is assumed. Resonances are found which would be absent for a strictly local skin-effect condition and which satisfactorily account for observed resonances that have been previously attributed to spin and combination resonances.

I. INTRODUCTION

SMITH, Hebel, and Buchsbaum[1] (SHB) have reported the results of microwave experiments on pure, single-crystal bismuth. They measured the power absorption coefficient as a function of static magnetic field **B** for radiation propagating normal to the surface of a slab of sample with **B** parallel to the sample surface. The results were analyzed in terms of a semiclassical theory[2] which was based on assumption of a strictly local relation between the microwave electric field **E** and the induced current **J**.

The local theory explained the most prominent features of the results. For **E** polarized perpendicular to **B** the power absorption was characterized by onsets of absorption at hybrid resonances. Such singularities correspond to resonances in the electron-hole plasma involving several types of carriers and result from the longitudinal space-charge field which is present for $\mathbf{E}\perp\mathbf{B}$. For **E** polarized parallel to **B** the power absorption displayed peaks which resulted from cyclotron resonance for those carriers whose orbits were tilted with respect to **B**—so-called longitudinal or tilted-orbit cyclotron resonance. Only for such carriers does **E** have a component in the plane of the orbit, which can couple to the cyclotron motion.

Additional singularities were also observed which were not accounted for by the local theory. They occurred when the microwave frequency ω equaled the cyclotron frequency ω_c and in some instances when $\omega\cong 2\omega_c$. Such singularities were especially pronounced for **E** parallel to **B** for carriers whose orbits were perpendicular to **B** and which could *not*, as a result, display a cyclotron resonance in a local theory. SHB tentatively attributed such singularities to spin resonances or combination resonances of the sort discussed by Cohen and Blount.[3] However, a later calculation by Hebel, Blount, and Smith[4] given in the immediately preceding article, showed that the size of singularities due to spin resonance could not possibly be great enough to explain the experimental results, even taking into account the large g factors expected in bismuth.

It will be shown in this paper that singularities having the proper size and shape result naturally from the theory if the strictly local relation between **J** and **E** is relaxed to allow small nonlocal terms.[5] The nearly local limit has often been referred to as the anomalous relaxation limit.[6] It has been studied recently by Jones and Sondheimer[7] for carriers with spherical Fermi surfaces with results presented for infinite carrier relaxation times. The theory to be presented here calculates the motion of individual carriers with a method, based on Hamilton's equations adapted to the bismuth band structure, in which the relaxation time plays an important role. The quantitative discussion will be limited to the case of **E** parallel to **B** where the largest nonlocal effects were observed. The singularities which result are also quite different in shape from those which have been calculated for the extreme anomalous limit.[8,9]

To calculate the power absorption one must solve the wave equation

$$\nabla\times(\nabla\times\mathbf{E})-(\omega/c)^2[\epsilon_l\mathbf{E}+(4\pi/i\omega)\mathbf{J}]=0, \qquad (1)$$

where ϵ_l is the dielectric constant of the lattice. If a local $\mathbf{J}(\mathbf{E})$ is used, then $\mathbf{J}=\boldsymbol{\sigma}\cdot\mathbf{E}$ which results in an exponential solution; for a wave propagating in the x direction $\mathbf{E}(x,t)=\mathbf{E}\exp i(\omega t-kx)$. The power absorption coefficient A is given in general in terms of the ratio of the microwave magnetic field **H** to **E** at the surface, obtained by solving the boundary conditions for propaga-

[1] G. E. Smith, L. C. Hebel and S. J. Buchsbaum, Phys. Rev. **129**, 154 (1963).
[2] The same theory has been used to analyze experiments with **B** perpendicular to the surface. See J. K. Galt, W. A. Yager, F. R. Merritt, B. B. Cetlin and A. D. Brailsford, Phys. Rev. **114**, 1396 (1959).
[3] M. H. Cohen and E. I. Blount, Phys. Mag. **5**, 115 (1960).
[4] L. C. Hebel, E. I. Blount, and G. E. Smith, preceding paper, Phys. Rev. **138**, A1636 (1965).
[5] Nonlocal effects in bismuth have been considered for **B** perpendicular to the surface by P. B. Miller and R. R. Haering, Phys. Rev. **128**, 126 (1962), and by J. Kirsch, Phys. Rev. **133**, A 1390 (1964). The Doppler shifts characteristic of their geometry are absent for **B** parallel to the surface.
[6] A. B. Pippard, Adv. Electron. Electron Phys. **6**, 1 (1954).
[7] M. C. Jones and E. H. Sondheimer, Proc. Roy. Soc. (London) **A278**, 256 (1964).
[8] M. Ia. Azbel' and E. A. Kaner, Zh. Eksperim. i Teor. Fiz. **30**, 811 (1956) [English transl.: Soviet Phys.—JETP **3**, 772 (1956)]; J. Phys. Chem. Solids **6**, 113 (1958); D. C. Mattis and G. Dresselhaus, Phys. Rev. **111**, 403 (1958); S. Rodriguez, *ibid.* **112**, 1616 (1958).
[9] As an experimental example, see A. F. Kip, D. N. Langenberg, and T. W. Moore, Phys. Rev. **124**, 359 (1961); J. E. Aubrey and R. G. Chambers, J. Phys. Chem. Solids **3**, 128 (1957).

tion normal to a slab. That is,

$$A=4n/[(n+1)^2+\kappa^2], \tag{2}$$

where $n=\mathrm{Re}(H/E)$ and $\kappa=\mathrm{Im}(H/E)$. Here, n and κ may be regarded as the real and imaginary parts of the surface admittance; in local theory they are also the real and imaginary parts of the index of refraction.

In the nearly local limit $\mathbf{J}(\mathbf{r})$ is determined by fields in the immediate vicinity of $\mathbf{r}$, so that it is attractive to expand $\mathbf{J}$ in a power series involving $\mathbf{E}$ and its derivatives. If only the terms up to second derivative are kept, the wave equation can still be solved easily, and one obtains the best self-consistent exponential field. It will be shown that such terms give resonances at $\omega=\omega_c$ which describe those observed by SHB. Proper treatment of carriers which collide with the surface is important and can easily be done to lowest order. Higher derivatives of $\mathbf{E}$ give resonances at $\omega=n\omega_c$ some of which are seen by SHB. Such resonances will only be discussed qualitatively.

A brief discussion of the bismuth band structure is given in Sec. II. In Sec. III the current density is calculated both for carriers in the bulk and for carriers whose orbits strike the surface. The calculation of the power absorption coefficient follows in Sec. IV, and in Sec. V the results are used to discuss the resonances observed by SHB.

II. BAND-STRUCTURE ASSUMPTIONS

In bismuth,[10] the carriers are believed to be characterized by Fermi surfaces which are ellipsoidal in cross section but nonparabolic in energy $\mathcal{E}$ versus momentum $\mathbf{p}$. A model of the band structure has been introduced by Lax *et al.*[11] which has been highly successful in interpreting infrared absorption phenomena. In the model the nonparabolicity is such that for calculations of the microwave frequency current a conventional parabolic relation may be substituted for $\mathcal{E}(\mathbf{p})$ provided the inverse effective masses used are those evaluated at the Fermi energy $\mathcal{E}_0$. Such a parabolic form will be assumed in this article; it is identical to that conventionally used to interpret de Haas–van Alphen, transport, and cyclotron resonance experiments in bismuth.

A Cartesian coordinate system is chosen in which axis 1 lies along a binary axis of the crystal, axis 2 along a bisectrix axis and axis 3 along the trigonal axis. The electron band is made up of three ellipsoids slightly tilted out of the plane perpendicular to the threefold axis. For a typical ellipsoid, to be referred to as ellipsoid "a," the electron energy is given by[10]

$$2\mathcal{E}=\alpha_1 p_1^2+\alpha_2 p_2^2+\alpha_3 p_3^2+2\alpha_4 p_2 p_3, \tag{3}$$

where $\mathbf{p}$ is measured relative to the ellipsoid center and the α's are components of the reciprocal mass tensor. For such an ellipsoid, the mass tensor itself has the form

$$\mathbf{m}_a/m_0=\begin{bmatrix} m_1 & 0 & 0 \\ 0 & m_2 & m_4 \\ 0 & m_4 & m_3 \end{bmatrix}. \tag{4}$$

The remaining electron ellipsoids, to be referred to as ellipsoids "b" and "c", are obtained by rotations of ellipsoid "a" through $\pm 120°$ about the trigonal axis.

The hole band is made up of an ellipsoid of revolution about the trigonal axis. Thus, for holes[10]

$$2(\mathcal{E}-\mathcal{E}_b)=(1/M_1)(p_1^2+p_2^2)+p_3^2/M_3, \tag{5}$$

where $\mathcal{E}_b$ is the band overlap energy. Where they are needed, values listed by SHB will be used: $m_1=0.0062$, $m_2=1.30$, $m_3=0.017$, $m_4=-0.085$, $M_1=0.057$, $M_3=0.77$.

III. CALCULATION OF THE CURRENT DENSITY

A. Basic Equations

When its Fermi frequency $\mathcal{E}_0/\hbar$ is much greater than the experimental frequency ω and the cyclotron frequency ω_c, a species of carrier in the metal is usually described by a semiclassical one-electron method. One formalism[12] uses a distribution function calculated using the Boltzmann equation. An equivalent but perhaps more direct method for situations of interest here is to calculate the motion of individual carriers using Hamilton's equations; impurity and wall scattering can be introduced when the current is evaluated. For a particle with charge e, momentum $\mathbf{p}$, and energy $\mathcal{E}=\mathcal{E}(\mathbf{p})$, Hamilton's equations yield

$$d\mathbf{p}/dt=e[\mathbf{E}e^{i\omega t}+(1/c)\mathbf{v}\times\mathbf{B}], \tag{6}$$

where

$$\mathbf{v}=\partial\mathcal{E}/\partial\mathbf{p}. \tag{7}$$

The current density is then obtained by averaging the velocity at $\mathbf{r}$ and t for a Fermi distribution over all orbits which pass through the point at that time. With the average denoted by $\langle\mathbf{v}\rangle$,

$$\mathbf{J}(\mathbf{r},t)=ne\langle\mathbf{v}\rangle=\mathbf{J}(\mathbf{r})e^{i\omega t}. \tag{8}$$

$\mathbf{E}$ and $\mathbf{B}$ will be taken parallel to each other and to the surface of a semi-infinite slab of metal. For convenience their direction is called the z direction which is taken along one of the principal directions of the mass-ellipsoid of the group of carriers being considered. Such a choice eliminates the tilted-orbit cyclotron resonance characteristic of the local theory for $\mathbf{E}$ parallel to $\mathbf{B}$, which otherwise masks the nonlocal effects for $\omega\simeq\omega_c$ and also is the most important case for analysis of the experimental results; a qualitative discussion is given in Sec. V for the case in which z is not along a principal direction.

[10] For extensive references; a general review of the properties and band structure of bismuth, see W. S. Boyle and G. E. Smith, *Progress in Semiconductors*, Vol. 7 (John Wiley & Sons, Inc., New York, 1963).

[11] B. Lax, J. G. Mavroides, H. J. Zeiger, and R. J. Keys, Phys. Rev. Letters **5**, 241 (1960); R. N. Brown, J. G. Mavroides, and B. Lax, Phys. Rev. **129**, 2055 (1963).

[12] See, for example, R. G. Chambers, Proc. Roy. Soc. (London) **A202**, 378 (1950); Proc. Phys. Soc. (London) **A65**, 458 (1952).

Propagation is taken along the x direction which is perpendicular to the face of the slab and which is *not* assumed to be along a principal mass-ellipsoid direction. Hence, the energy $\mathcal{E}(\mathbf{p})$ has the form

$$2\mathcal{E}=\alpha_x p_x^2+\alpha_y p_y^2+2\alpha_{xy}p_x p_y+\alpha_z p_z^2=2\mathcal{E}_1+\alpha_z p_z^2, \quad (9)$$

where α_i are inverse effective masses evaluated for $\mathcal{E}=\mathcal{E}_0$, the Fermi energy, and $\mathcal{E}_1$ is the energy of motion perpendicular to **B**.

Because **E** and **B** are taken to lie along a principal mass direction, $v_z=\alpha_z p_z$, so that Eq. (6) for p_z separates from the equations for p_x and p_y. A formal solution for a given particle may be written down immediately in terms of an integral back in time along its orbit. The contribution at time t from each earlier time t' must be weighted by the probability that no scattering due to bulk impurities has occurred in the time interval $t-t'$. Collisions with the walls are treated separately in Sec. III-D. Introducing a relaxation time τ to represent scattering by impurities in the metal, one has

$$v_z(x,t)=e\alpha_z\int_0^\infty \frac{d(t-t')}{\tau}\exp\left[-\frac{1}{\tau}(t-t')\right] \times\int_{t'}^{t} dt_1 E(x_1)\exp(i\omega t_1). \quad (10)$$

In order to proceed, we will make the approximation that $E(x_1)$ varies only slightly over the orbit in the (x,y) plane (see Sec. I). Thus $E(x_1)$ is expanded in a Taylor's series about the point x

$$E(x_1)=\sum_m \frac{1}{m!}\frac{d^m E}{dx^m}\bigg|_x (x_1-x)^m, \quad (11)$$

where in practice only the first few terms will be used. With

$$\bar{\tau}=\tau/(1+i\omega\tau) \quad (12)$$

and

$$\theta=\omega_c(t-t_1), \quad (13)$$

Eq. (10) may be partially integrated and combined with Eqs. (8) and (11) to give the desired equation for the current density,

$$J_z(x)=\frac{ne^2\alpha_z}{\omega_c}\sum_m\frac{1}{m!}\frac{d^m E}{dx^m} \times\left\langle\int_0 d\theta(x_1-x)^m\exp[-\theta\omega_c\bar{\tau}]\right\rangle, \quad (14)$$

where the upper limit is ∞ for orbits which do not strike the wall.

B. Solution of the Orbit

Evaluation of Eq. (14) for the current density requires solution of the orbit in the (x,y) plane. Relative to the center at $(\bar{x},\bar{y})$ the orbit is obtained by direct integration of Eq. (6) to obtain $(x-\bar{x})$ and $(y-\bar{y})$ in terms of p_x and p_y; substitution of the result in Eq. (9) gives the orbit equation

$$2\mathcal{E}_1(c/eB)^2=\alpha_y(x-\bar{x})^2 +\alpha_x(y-\bar{y})^2-2\alpha_{xy}(x-\bar{x})(y-\bar{y}), \quad (15)$$

which is an ellipse rotated 90° from that of the momentum ellipsoid and scaled by (c/eB).[2]

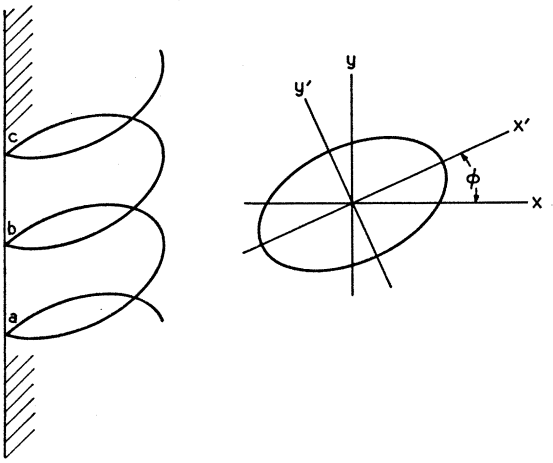

FIG. 1. Orbit of a carrier in real space with laboratory axes (x,y) and principal axes (x',y').

To evaluate the current, Eq. (14), only distances along the x direction of propagation are needed. Consequently, it is most convenient to transform to a system of coordinates in which the orbital motion is circular and in which distances in the x direction have a simple functional dependence. The details of the transformation are given in Appendix I. First a rotation is made about the z axis through the angle Φ, shown in Fig. 1, to x' and y' along principal directions of the orbit ellipsoid. Next a transformation is made to coordinates u_1 and u_2 shown in Fig. 2 by a shrink (or stretch) of axes followed by a rotation through an angle λ. Measuring u_1 and u_2 relative to the orbit center, the resulting motion is circular with a cyclotron frequency ω_c, an inverse cyclotron mass α_c, and an equivalent cyclotron radius r_c. That is,

$$\omega_c=eB\alpha_c/c \quad \text{with} \quad \alpha_c=(\alpha_x'\alpha_y')^{1/2}. \quad (16)$$

The orbit is given by

$$u_1^2+u_2^2=r_c^2=2\mathcal{E}_1\alpha_c/\omega_c^2, \quad (17)$$

where, as shown in Fig. 2, u_1 and u_2 can be simply expressed in terms of the angle ψ whose time derivative is a constant equal to ω_c.

$$u_1=r_c\cos\psi, \quad u_2=r_c\sin\psi. \quad (18)$$

In addition, the equation for $(x-\bar{x})$, the extent of the orbit along the propagation direction, becomes a simple

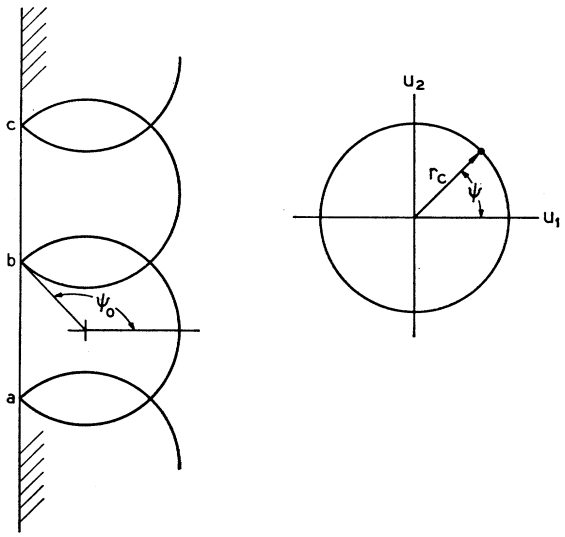

FIG. 2. Transformed orbit equation in (u_1,u_2) space.

one.

$$(x-\bar{x})=(\alpha_x/\alpha_c)^{1/2}u_1=(2\mathcal{E}_1\alpha_x/\omega_c^2)^{1/2}\cos\psi. \quad (19)$$

One notes that α_x in Eq. (19) is the inverse mass component along the propagation direction (in the lab system) and that the "tilt" of the orbit ellipsoid does not appear in the final equation for $(x-\bar{x})$.

C. Current Density for Carriers in the Bulk

For a carrier which does not strike the surface, the distance x_1-x back along the orbit may be taken as

$$x_1-x=(x_1-\bar{x})-(x-\bar{x})$$
$$=(2\mathcal{E}_1\alpha_x/\omega_c^2)^{1/2}[\cos(\psi+\theta)-\cos\psi] \quad (20)$$

where θ is defined in Eq. (13) and the angle ψ, shown in Fig. 2, is used to label the x coordinate at time t. The average over all orbits that arrive at the point (x,y) at the time t may then be regarded as an average over ψ combined with an average over the Fermi distribution. One finds

$$\langle x_1-x\rangle=0, \quad (21)$$

$$\langle(x_1-x)^2\rangle=(4\mathcal{E}_0\alpha_x/5\omega_c^2)(1-\cos\theta). \quad (22)$$

Thus for carriers in the bulk, substitution of Eq. (22) into Eq. (14) gives

$$J_z(x)\cong ne^2\alpha_z\bar{\tau}\left[E(x)+\frac{2}{5}\frac{\mathcal{E}_0\alpha_x}{\omega^2}\frac{\omega^2\bar{\tau}^2}{(1+\omega_c^2\bar{\tau}^2)}\frac{d^2E}{dx^2}\right]. \quad (23)$$

One notes that $d^2E/dx^2\sim E/\delta^2$ where δ is the skin depth; consequently, the second term in Eq. (23) is of order $(r_c/\delta)^2$ multiplied by a resonant factor compared to the first. As a result, the relaxation time must be finite and not too large for the theory to apply for ω near ω_c.

Higher terms in the expansion of $\mathbf{E}$ give additional resonances; a term of order $d^{2n}E/dx^{2n}$ contains a denominator $(1+\omega_c^2\bar{\tau}^2)(1+4\omega_c^2\bar{\tau}^2)\cdots(+n^2\omega_c^2\bar{\tau}^2)$. Thus, there are resonant terms at $\omega=2\omega_c$, $\omega=3\omega_c$, etc., with diminishing amplitudes if the series converges. The difficulty in treating these higher order terms is the labor required to calculate the current contribution to the proper order for those carriers which strike the surface as well as the increased complexity of the wave equation. The theory of this paper will be limited to a quantitative discussion of terms to order d^2E/dx^2. Higher terms will be considered only in a qualitative way. However, it should be noted that their resonant denominators have the same type of frequency dependence as the lowest order terms.

D. Current Density of Carriers Which Strike the Surface

For carriers which strike the surface $\langle x_1-x\rangle$ is no longer zero as it was for bulk carriers. However, the additional current density extends only a distance of order r_c into the metal whereas the bulk currents extend a skin depth δ. Since the $\langle x_1-x\rangle$ current density will be proportional to $r_c dE/dx\sim Er_c/\delta$, its net effect will be of the same order as the $\langle(x_1-x)^2\rangle$ contribution for bulk carriers, i.e., of order $E(r_c/\delta)^2$. Consistent with the approximation that $r_c\ll\delta$, the $\langle x_1-x\rangle$ contribution will be treated as a surface current. That is, one introduces the current per unit length Γ_z, where

$$\Gamma_z=\int_0^\infty dx J_z(x), \quad (24)$$

and defines

$$J_z'=\Gamma_z\delta_+(x). \quad (25)$$

J_z' will then be used instead of J_z itself for the contribution of the $\langle x_1-x\rangle$ term. The difference between the two involves terms of higher order than $(r_c/\delta)^2$ which are dropped.

The equation for the surface is a simple one in the u_1, u_2 system. Referring to Fig. 2, the wall at x_0 can be specified in terms of the angle ψ_0. Using Eq. (19) one has

$$x_0=(2\mathcal{E}_1\alpha_x\omega_c^2)^{1/2}\cos\psi_0. \quad (26)$$

1. *Diffuse Reflection*

For diffuse reflection, one assumes a complete loss of phase memory with a surface collision.[13] Thus, in evaluating Eq. (14) for J_z, the integration is carried out over the angle θ only until the particle in question strikes the wall. The resulting expression is then averaged for a Fermi distribution over all orbits which strike the surface. To obtain Γ_z, Eqs. (14), (20), (24), and (26) must be combined. The details are given in Appendix II. After averaging over the Fermi distribution the final

[13] For more extensive discussion of treatment of boundary scattering, see P. J. Price, IBM J. Res. Develop. 4, 152 (1952).

result is

$$J_z'(x)=ne^2\alpha_z\left[\tfrac{2}{5}(\mathcal{E}_0\alpha_x/\omega^2)\left(\frac{dE}{dx}\right)_0 \times\omega^2\bar{\tau}^2/(1+\omega_c^2\bar{\tau}^2)\right]\delta_+(x). \quad (27)$$

2. *Specular Reflection*

When the particle is specularly reflected its energy is conserved. For a "specular force" normal to the surface, Eq. (6) shows that p_y parallel to the surface is also conserved.[13] Then direct integration of Eq. (6) shows that the x coordinate of the orbit relative to the orbit center is unchanged by the collision. This means that, in Figs. 1 and 2, after striking the wall at "b," the particle starts toward "c" with the same p_x and p_y that it had at "a." The orbit thus remains the same except that it is displaced in the y direction with successive collisions. Since the phase of $\mathbf{E}$ is not a function of y, the problem can be simplified by putting the particle back at "a" when it strikes the wall at "b," making the orbit re-entrant. However, the angle θ in Eq. (14) for J_z must then be increased by $2(\pi-\psi_0)$ with each successive collision.

Consequently, in addition to the term J_z' calculated in Eq. (27), one must continue the integration over all paths between successive wall collisions to obtain a second contribution. This second portion is shown in Appendix II to be identically zero to order $(r_c/\delta)^2$ because contributions at the surface are 180° out of phase to contributions at distances of order r_c. Thus, to order $(r_c/\delta)^2$ both specular and diffuse scattering give the same result for J_z'.

IV. ABSORPTION COEFFICIENT FOR *E* PARALLEL TO *B*

In this section it will be shown that under slightly nonlocal conditions the absorption coefficient A displays a resonance for $\omega\cong\omega_c$ whose shape is predominantly that of either a classical absorption or dispersion, depending on whether the real part of the total dielectric constant is negative or positive. To calculate A given by Eq. (2), the ratio of $\mathbf{H}$ to $\mathbf{E}$ at the surface must be obtained by solving the wave equation, Eq. (1), using a current density given by the sum of Eqs. (23) and (27) for all the carriers. Since the nonlocal terms are only appreciable near a resonance for $r_c\ll\delta$, such terms will be kept only for that carrier for which $\omega\cong\omega_c$, with only the usual local term kept for all other carriers.

It is convenient to write the current density contributions to the wave equation in terms of equivalent dielectric constants ϵ_1 and ϵ_T, where ϵ_1 includes only terms from the resonant group of carriers and ϵ_T terms from all carriers. Including the "lattice" dielectric constant ϵ_l, one uses

$$\epsilon_1=4\pi ne^2\alpha_z\bar{\tau}/i\omega=\omega_p^2\bar{\tau}/i\omega, \quad (28)$$

and

$$\epsilon_T=4\pi ne^2\sum_j n_j\alpha_{zj}\bar{\tau}/i\omega+\epsilon_l=\Omega_p^2\bar{\tau}/i\omega+\epsilon_l, \quad (29)$$

where ω_p is the plasma frequency for the resonant carriers and Ω_p is the total plasma frequency. The nonlocal character of the resonant terms can be expressed to order $(r_c/\delta)^2$ by a parameter ξ which is basically a resonant factor times the ratio of the Fermi velocity to the velocity of light. That is, for the resonant carriers, one introduces

$$\xi=\frac{2}{5}\frac{\mathcal{E}_0\alpha_x}{c^2}\frac{\omega^2\bar{\tau}^2}{(1+\omega_c^2\bar{\tau}^2)}. \quad (30)$$

Substitution of the current density, Eqs. (23) and (27) into the wave equation then gives the basic equation for E to order $(r_c/\delta)^2$.

$$(1+\epsilon_1\xi)d^2E/dx^2+(\omega/c)^2\epsilon_TE +\epsilon_1\xi(dE/dx)_0\delta_+(x)=0. \quad (31)$$

Thus, inside the metal the field to second order varies exponentially with a propagation constant given by

$$(ck/\omega)^2=\epsilon_T/(1+\epsilon_1\xi). \quad (32)$$

In addition, dE/dx and hence H have a discontinuity at the surface due to the fact that the current contributions from electrons which strike the surface has been treated as a surface current. Equation (31) shows that

$$(d/dx)[(1+\epsilon_1\xi)(dE/dx)+\epsilon_1\xi(dE/dx)_0U_+(x)]|_0=0, \quad (33)$$

where $U_+(x)$ is a unit step function. Using Maxwell's equations to relate E to H and labeling H just inside or just outside the surface as H_i and H_o, respectively, the solution of Eq. (33) is

$$H_o/H_i=1+\epsilon_1\xi. \quad (34)$$

Combining Eqs. (32) and (34), one finds for η, the ratio of H to E just outside,

$$\eta^2=(H_o/H_i)^2(ck/\omega)^2=\epsilon_T(1+\epsilon_1\xi). \quad (35)$$

The solutions for both η and A are most conveniently expressed in terms of a dimensionless frequency difference Δ and linewidth γ, in addition to a carrier Fermi velocity v_{0x}, given by

$$\Delta=(\omega_c-\omega)/\omega, \quad (36)$$

$$\gamma=1/\omega\tau, \quad (37)$$

$$v_{0x}=2\mathcal{E}_0\alpha_x. \quad (38)$$

Recalling that $\bar{\tau}=\tau(1+i\omega\tau)$ and $\eta=n-i\kappa$, substitution of Eqs. (28)–(30) into Eq. (35) gives the desired result for η^2. Dropping the "lattice" term, ϵ_l, at microwave

frequencies,

$$\eta^2=n^2-\kappa^2-2in\kappa$$
$$\cong-\frac{\Omega_p^2}{\omega^2}(1+i\gamma)\left[1-\frac{1}{10}\frac{v_{0x}^2}{c^2}\frac{\omega_p^2}{\omega^2}\frac{(1+i\gamma)(\Delta-i\gamma)}{(\Delta^2+\gamma^2)}\right]. \quad (39)$$

Since $\gamma\ll 1$ and the nonlocal contribution in the square bracket is regarded as small, one finds $\kappa\cong\Omega_p/\omega$ and $n\cong\Omega_p\gamma/2\omega$ (which is the local result), so that $\kappa\gg n$. Thus from Eq. (2) the power absorption is very small; $A\cong 4n/\kappa^2$, so that the sample is said to be "cut-off." Since the "local" skin depth, δ_0, would be given by $\delta_0=(\omega\kappa/c)\cong\Omega_p/c$, the nonlocal term in Eq. (39) is seen to be of order $(r_c^2/10\delta_0^2)$ multiplied by a resonant factor when $\omega\cong\omega_c$. Including the nonlocal terms, one has

$$A\cong\left(\frac{2\omega\gamma}{\Omega_p}\right)\left[1+\frac{1}{10}\frac{v_{0x}^2}{c^2}\frac{\omega_p^2}{\omega^2}\frac{(1-\frac{1}{2}\Delta)}{(\Delta^2+\gamma^2)}\right] \quad (40)$$

which is schematically plotted in Fig. 3.

The local case, obtained by setting $v_{0x}=0$ in Eq. (40), shows no resonance for **E** parallel to **B** along a principal axis since there is no coupling between **E** and the cyclotron motion. However, the nonlocal effect to order $(r_c/\delta)^2$ contributes resonant terms of both "dispersive" shape and "absorptive" shape. Since the maximum value of $\Delta/(\Delta^2+\gamma^2)\cong 1/\gamma$, one notes that the power absorption A near $\Delta=0$ has a Lorentz line shape which is predominantly "absorptive" with a little "dispersion" mixed in, of order $\gamma=1/\omega\tau\ll 1$. The peak of the resonance occurs for ω very close to ω_c. Such a shape results from the almost cut-off condition since the dispersive term must compete with unity whereas the absorptive term must compete with $\gamma\ll 1$.

At sufficiently high frequencies the "lattice" dielectric constant must be taken into account. In fact, when $\epsilon_l>\Omega_p^2/\omega^2$, Eqs. (35)–(39) show that in the local theory $n^2=\epsilon_l-\Omega_p^2/\omega^2$ whereas $\kappa\cong\Omega_p^2\gamma/2n$; consequently, $n\gg\kappa$, and the sample "opens up." Under such circumstances the nonlocal terms give a resonance which is predominantly dispersive with a little absorption mixed in, just the reverse of the low-frequency shape. Thus when the nonlocal terms are small, the shape will be determined by whether the real part of the total dielectric constant is positive or negative.

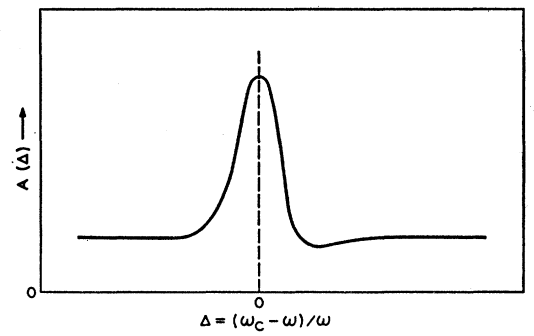

FIG. 3. Plot of power absorption $A(\Delta)$ versus $\Delta=(\omega_c-\omega)/\omega$ from Eq. (40).

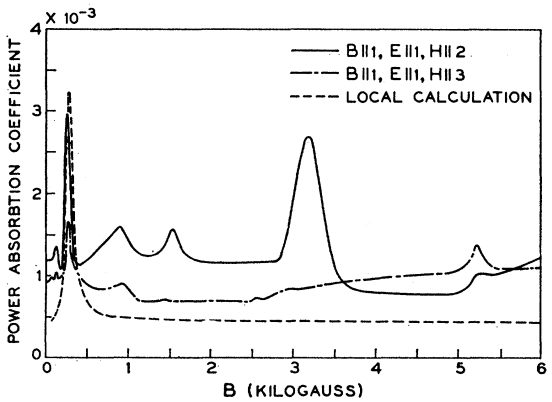

FIG. 4. Observed power absorption versus magnetic field for **B** and **E** along axis 1 (binary); the propagation vector **k** is along either axis 2 (bisectrix) or axis 3 (trigonal) (from Ref. 1).

V. RESONANCE IN BISMUTH

The experimental power absorption coefficient A, measured by SHB as a function of **B**, is shown in Fig. 4 for **B** and **E** along axis 1 (binary); the propagation vector **k** is along either axis 2 (bisectrix) or axis 3 (trigonal). The resonance at about 250 G was identified by SHB as a tilted-orbit cyclotron resonance (see Sec. I) which is due to electrons in ellipsoids "*b*" and "*c*."

At approximately 3.15 kG there is a resonance which is very large for **k** along axis 3 but almost absent for **k** along axis 2. It occurs at the cyclotron frequency for electrons in ellipsoid "*a*." Since this ellipsoid is *not* tilted with respect to **B** for **B** along axis 1, the nonlocal theory offers no explanation. Careful experimental orientation studies showed that the observed resonance did not result from misorientation of either **B** or **E** with respect to axis 1, and yet could definitely be attributed to electrons in ellipsoid "*a*" because of the known mass anisotropy. Consequently, the resonance was tentatively attributed by SHB to electron spin resonance of the sort suggested by Cohen and Blount. However, later calculations of the spin resonance intensity by Hebel, Blount, and Smith,[4] given in the immediately preceding article, show that the observed line is much too "strong" by at least two orders of magnitude to be due to spin resonance.

The theory with a lightly nonlocal current-field relation offers an excellent explanation of the 3.15 kG resonance. As can be seen by comparing Figs. 3 and 4, the line shape is as predicted by Eq. (40), an absorptive shape with a slight dispersive character; the amount of dispersion is that appropriate to a line width factor $\gamma\cong 1/20$ and has the proper sign to agree with Eq. (40).

In addition, the size of the change in A is approximately that predicted by the theory for **k** parallel to

axis 3. Referring to Eqs. (28), (37), (38), and (40), with $\mathcal{E}_0=25$ meV, $\alpha_z\cong 160$, $\alpha_x\cong 90$, and $\omega=4.4\times 10^{11}$ per sec (4.3 mm), one finds

$$\frac{1}{10}\frac{v_{0x}^2}{c^2}\frac{\omega_p^2}{\omega^2}\cong 0.2,$$

and at the peak

$$A(\omega\cong\omega_c)=2\times 10^{-3}. \tag{41}$$

Thus, the current-field relation is barely local in the wings of the line; the resonant factor results in a violation of $r_c\ll\delta$ when $\omega\cong\omega_c$ for this orientation of **B** and **k**. While more terms in the series would be necessary accurately to predict the size of the line under these circumstances, the peak height, estimated in Eq. (41), is approximately verified.

Moreover, the line is almost absent for **k** parallel to axis 2. Such an effect is also predicted by the theory. The nonlocal terms are proportional to v_{0x}^2 which is proportional α_x [See Eq. (38).] For **k** parallel to axis 3, where the resonance is large, $\alpha_x\cong 90$; on the other hand for **k** parallel to axis 2, α_x becomes of order unity resulting in a correspondingly smaller resonance.

Still in reference to Fig. 4, the resonance at 1.55 kG is identified as the 2nd harmonic resonance of the 3.15 kG line due to higher terms in the expansion of the slightly nonlocal electric field. An accurate calculation of its size involves a much more accurate treatment of the current due to electrons which strike the surface, and a quantitative estimate will not be made here. The line at 5.25 kG is identified as a resonance due to holes, resulting from the slightly nonlocal electric field. The size is close to that estimated using Eqs. (28), (37), (38), and (40) with $\mathcal{E}_0\cong 8$ meV and the mass parameters of SHB. The 3.15 and 5.25 kG resonances give the following cyclotron masses for the hole ellipsoid and electron ellipsoid a with **B** parallel to axis 1:

for electrons,

$$m_a=0.126m_0;$$

for holes,

$$M=0.210m_0.$$

The value of M is that given by SHB and differs from that of Galt[2] by 18%. The value of m_a lies between those of SHB and Galt, differing from either one by 3%. These cyclotron mass values, obtained from the peaks of the two resonances, should be quite accurate since the fractional width and the accompanying dispersive shift are small.

The remaining resonance of Fig. 4 at approximately 900 G is believed to be a spurious one due to a slight sample misalignment. It occurs at the same field value as the large tilted-orbit cyclotron resonance shown in Fig. 5 for **B** and **E** along axis 2 (bisectrix). In Fig. 5, one also notes a small resonance at 5.25 kG which is attributed to cyclotron resonance of the holes due to

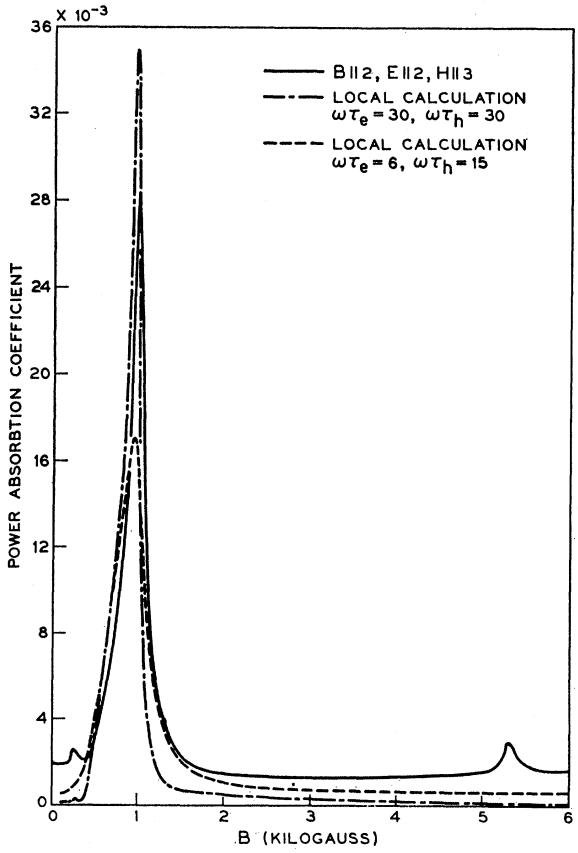

FIG. 5. Observed power absorption versus magnetic field **B** for **B** and **E** along axis 2 (bisectrix) (from Ref. 1).

nonlocal terms. The resonance field is exactly the same as for **B** along axis 1, in agreement with the assumed model for the hole momentum ellipsoid.

There are additional small resonances of nonlocal origin in Fig. 5 at fields just below the onset of absorption ($\omega\cong\omega_c$) for the large tilted-orbit cyclotron resonance. As discussed in preceding sections, such a cyclotron resonance occurs for **E** parallel to **B** in a local theory only when **B** is not along a principal axis of the mass ellipsoid. The calculation on nonlocal terms in such a case is more difficult than that presented in Sec. III, since the z motion is coupled to the x-y motion even in first order. In the local theory the dielectric constant is very large near $\omega\cong\omega_c$; thus the phase velocity would be low which is the very condition in which nonlocal terms are important. The fact that the observed nonlocal resonances are small is undoubtedly due to the large dielectric constant for $\omega\cong\omega_c$; the resulting absorption coefficient is very small and the sample remains essentially "cutoff" even with additional nonlocal terms.

Several other figures in SHB, dealing with resonances in the geometry of $\mathbf{E}\perp\mathbf{B}$, will not be reproduced here. The dominant effects were due to hybrid resonances, as discussed in Sec. I. There are small resonances present in the curves which were tentatively attributed to spin

and combination resonances but which are now believed to be due to small nonlocal terms. In the hybrid geometry the analysis is considerably complicated by the fact that the electric field inside the sample is elliptically polarized in such a way that resonance at $\omega=\omega_c$ does not normally appear in a local theory. It can be shown that such is the case even with nonlocal terms to order $(r_c/\delta)^2$.

As a result, the nonlocal effects in the hybrid geometry have important contributions from terms of order higher than $(r_c/\delta)^2$, which also give rise to the observed resonances at subharmonics of ω_c. Such resonances call for more accurate treatment of the currents near the surface than is attempted in this paper. However, the results would be qualitatively similar to what is expected from the discussion presented in Sec. IV, that is, lines at subharmonics which are predominantly absorptive in shape when $n\ll\kappa$ (absorption A cutoff) and predominantly dispersive in shape when $n\gg\kappa$.

ACKNOWLEDGMENTS

It is a pleasure to acknowledge a number of discussions concerning nonlocal effects with P. A. Wolff, M. Lax, S. J. Buchsbaum, G. E. Smith, P. M. Platzman, and E. I. Blount. The author is indebted to S. J. Buchsbaum and G. E. Smith for critical review of the manuscript.

APPENDIX A

The first transformation, shown in Fig. 1, is a rotation about the z axis through an angle Φ from laboratory (crystallographic) coordinates (x,y) to principle ellipsoid coordinates (x',y') and is given by

$$x-\bar{x}=(x'-\bar{x}')\cos\Phi-(y'-\bar{y}')\sin\Phi, \tag{A1}$$

$$y-\bar{y}=(y'-\bar{y}')\cos\Phi+(x'-\bar{x}')\sin\Phi, \tag{A2}$$

where $(\bar{x},\bar{y})$ and $(\bar{x}',\bar{y}')$ label the orbit center. The transformed momenta along the orbit are then given by transforming Eq. (9), so that

$$2\mathcal{E}_\perp=\alpha_{x'}p_{x'}{}^2+\alpha_{y'}p_{y'}{}^2=2\mathcal{E}-\alpha_z p_z{}^2, \tag{A3}$$

where

$$\alpha_x=\alpha_{x'}\cos^2\Phi+\alpha_{y'}\sin^2\Phi, \tag{A4}$$

$$\alpha_y=\alpha_{y'}\cos^2\Phi+\alpha_{x'}\sin^2\Phi, \tag{A5}$$

$$\alpha_{xy}=(\alpha_{x'}-\alpha_{y'})\sin\Phi\cos\Phi. \tag{A6}$$

Next one transforms to coordinates u_1 and u_2 shown in Fig. 2, as discussed in Sec. III, by choosing

$$x'-\bar{x}'=(\alpha_{y'})^{-1/2}(u_1\cos\lambda-u_2\sin\lambda), \tag{A7}$$

$$y'-\bar{y}'=(\alpha_{x'})^{-1/2}(u_2\cos\lambda+u_1\sin\lambda), \tag{A8}$$

where

$$\tan\lambda=-(\alpha_{y'}/\alpha_{x'})^{1/2}\tan\Phi. \tag{A9}$$

One then obtains a circular motion as discussed in Sec. III with a simple relation between distances along the propagation direction in the laboratory system and the orbital angle ψ in the (u_1,u_2) system, namely Eq. (19):

$$(x-\bar{x})=(2\mathcal{E}_\perp\alpha_x/\omega_c{}^2)^{1/2}\cos\psi. \tag{A10}$$

APPENDIX B

To obtain J_z', Eqs. (14), (20), (24), and (26) must be combined. For diffuse reflection the integration is performed over the angle θ only until the particle in question strikes the wall. The result depends on an integral I_{z1} over the path given by

$$I_{z1}=(2\pi)^{-1}(2\mathcal{E}_\perp\alpha_z\omega_c{}^2)^{1/2}\times\int_0^\infty dx\int_{-\pi}^{\pi}d\psi\int_0^{\psi-\psi_0}d\theta[\cos(\psi+\theta)-\cos\psi]\times\exp[-\theta/\omega_c\bar{\tau}]U[\cos\psi-\cos\psi_0], \tag{B1}$$

where $U[\cos\psi-\cos\psi_0]$ is a unit step function to restrict the orbit to be within the metal. I_{z1} is most easily evaluated by changing from dx to $d\psi_0$ using Eq. (26). The effect of the unit function can then be lumped into the limits of the integral over ψ from $-\psi_0$ to ψ_0. One finds

$$I_{z1}=(\mathcal{E}_\perp\alpha_z\omega_c\bar{\tau})/(1+\omega_c{}^2\bar{\tau}^2). \tag{B2}$$

After averaging Eq. (B2) over the Fermi distribution and combining the remaining constants from Eq. (14), the final result is that of Eq. (27), namely,

$$J_z'(x)=ne^2\alpha_z\left[\frac{2}{5}\frac{\mathcal{E}_0\alpha_x}{\omega^2}\frac{dE}{dx}\bigg|_0\frac{\omega^2\bar{\tau}^2}{(1+\omega_c{}^2\bar{\tau}^2)}\right]. \tag{B3}$$

For specular reflection, in addition to the term I_{z1} calculated in Eq. (B1), one must continue the integration over all paths between successive wall collisions to obtain a second contribution I_{z2}. This second portion may be shown to be identically zero to order $(r_c/\delta)^2$. Developing I_{z2} in a similar way to Eq. (43) one can use the reentrant orbit discussed in Sec. IIID2, except that the θ integration now runs from $\psi_0-\psi$ to ∞ and $\cos(\psi+\theta)$ changes by $2(\pi-\psi_0)$ with each collision. One has

$$I_{z2}\propto\int_0^\pi d\psi_0\int_{-\psi_0}^{\psi_0}d\psi\int_{\psi_0-\psi}^{\infty}d\theta[\cos(\psi+F(\theta))-\cos\psi]\times\exp[-\theta/\omega_c\bar{\tau}], \tag{B4}$$

where

$$F(\theta)=\theta+2(m+1)(\pi-\psi_0) \tag{B5}$$

for

$$\psi_0-\psi+2m\psi_0<\theta<\psi_0-\psi+2(m+1)\psi_0 \tag{B6}$$

with

$$m=0,\,1,\,2\cdots.$$

Thus the result for I_{z2} may be written as an infinite

series

$$I_{z2}\propto\sum_{m=0}^{\infty}\int_0^{\pi}d\psi_0\int_{-\psi_0}^{\psi_0}d\psi \times\int_a^b d\theta\{\cos[\psi+\theta+2(m+1)(\pi-\psi_0)] -\cos\psi\}\exp[-\theta/\omega_c\bar{\tau}], \quad \text{(B7)}$$

where $a=\psi_0-\psi+2m\psi_0$ and $b=\psi_0-\psi+2(m+1)\psi_0$. Changing variable,

$$\theta'=\theta-(\psi_0-\psi)-2m\psi_0,$$

one can sum the series as a binomial expansion of $[1-\exp(-2\psi_0/\omega_c\bar{\tau})]$. One finally obtains

$$I_{z2}\propto\int_0^{\pi}d\psi_0\int_0^{\psi_0}d\psi\frac{\cosh(\psi/\omega_c\bar{\tau})}{\sinh(\psi_0/\omega_c\bar{\tau})} \times\int_0^{2\psi_0}d\theta'[\cos(\theta'-\psi_0)-\cos\psi]\exp[-\theta'\omega_c\bar{\tau}]. \quad \text{(B8)}$$

The result in the form of Eq. (B8) may be shown to be identically zero because contributions to I_{z2} at the surface are 180° out of phase to contributions at distances of order r_c.

PHYSICAL REVIEW VOLUME 138, NUMBER 6A 14 JUNE 1965

Magnetization Distribution in a Palladium-Rich FePd Alloy*

WALTER C. PHILLIPS†
Department of Physics, Massachusetts Institute of Technology, Cambridge, Massachusetts
(Received 19 October 1964; revised manuscript received 1 February 1965)

A ferromagnetic $Fe_{0.013}$ $Pd_{0.987}$ single crystal was examined with the polarized-beam neutron-diffraction technique in a study of the distribution of the localized magnetization in the alloy. Intensities of all nineteen Bragg reflections out to $\sin\theta/\lambda=0.90$ Å^{-1} were measured at 4.2°K in a field of 14 kOe, yielding the magnetic form factor averaged over all atoms. These data are fitted to a linear combination of calculated 3*d* and 4*d* free-atom form factors, resulting in a moment of 0.050 ± 0.006 μ_B of 3*d*-like moment and 0.088 ± 0.008 μ_B of 4*d*-like moment per average atom. A Fourier inversion of the magnetic scattering amplitudes emphasizes the aspherical shape of the unpaired-electron distribution. The over-all E_g/T_{2g} ratio is 0.39 ± 0.02. The measured saturation magnetization of this alloy is 0.114 ± 0.004 μ_B per atom at 4.2°K, which is considerably smaller than the total moment of 0.138 μ_B seen by neutron diffraction. This discrepancy suggests a negative conduction-electron polarization of -0.024 ± 0.011 μ_B per atom. The temperature dependence of the magnetic scattering amplitude and the saturation magnetization indicate that the conduction-electron polarization disappears near the Curie temperature, which is about 55°K. In addition, these data suggest that the 3*d* moment on an Fe atom and the 4*d* moments on surrounding Pd atoms are strongly coupled, although the range of the Pd polarization is not determined. The total *d* moment associated with the moment cluster around each impurity site is 10.7 ± 0.6 μ_B.

INTRODUCTION AND THEORY

MANY alloys in which a 3*d* atom impurity is present in a 4*d* atom matrix exhibit interesting magnetic properties.[1–6] Dilute solutions of Fe in Pd are ferromagnetic at suitably low temperatures for all compositions which have been studied (except for an extremely dilute sample[7]) and apparently ferromagnetism will exist at fractional-percent Fe concentrations. An FePd alloy was chosen for this study because of the relatively high Curie temperature and large moment per Fe atom reported earlier.[3,5–7] (The measured Curie temperature is 55°K and the saturation magnetization is 8.8 ± 0.5 μ_B per Fe atom in our sample.) From these moment values it is evident that not only the Fe atoms contribute to the ferromagnetic moment, but each Fe impurity polarizes some Pd atoms, resulting in an enhanced moment per Fe atom. The large paramagnetic susceptibility[8] of pure Pd shows that the 4*d* bands are not filled, and apparently a ferromagnetic impurity can trigger the Pd matrix into a ferromagnet.

* This work was supported by a research grant from the U. S. Atomic Energy Commission. It is based on a thesis submitted to the Department of Physics at the Massachusetts Institute of Technology in May, 1964 in partial fulfillment of the requirements for the degree of Doctor of Philosophy.

† Present address: Argonne National Laboratory, Argonne, Illinois.

[1] M. Fallot, Ann. Phys. (Paris) **10**, 291 (1938).
[2] D. Gerstenberg, Ann. Physik **2**, 236 (1958).
[3] J. Crangle, Phil. Mag. **5**, 335 (1960).
[4] R. M. Bozorth, P. A. Wolff, D. D. Davis, V. B. Compton, and J. H. Wernick, Phys. Rev. **122**, 1157 (1961).
[5] R. M. Bozorth, D. D. Davis, and J. H. Wernick, J. Phys. Soc. Japan **17**, Suppl. BI, 112 (1962).
[6] A. M. Clogston, B. T. Matthias, M. Peter, H. J. Williams, E. Corenzwit, and R. C. Sherwood, Phys. Rev. **125**, 541 (1962).
[7] P. P. Craig, D. E. Nagle, W. A. Steyert, and R. D. Taylor, Phys. Rev. Letters **9**, 12 (1962).
[8] D. W. Budworth, F. E. Hoare, and J. Preston, Proc. Roy. Soc. **A257**, 250 (1960).